Radiation into transverse electric modes of rectangular waveguides from spatiotemporally modulated gyrating electron beams

J. L. Hirshfield
Omega-P, Inc., 2008 Yale Station, New Haven, Connecticut 06520
and Physics Department, Yale University, P.O. Box 6666, New Haven, Connecticut 06511
(Received 6 February 1992)

A previously published analysis [J. L. Hirshfield, Phys. Rev. A **44**, 6845 (1991)] of the first-order transfer of power into fields of a TE_{0m} rectangular waveguide from a relativistic electron beam carrying spatiotemporal modulation is extended to TE_{lm} modes. Non-axis-encircling orbits, circularly polarized excitations, and competing modes are incorporated into the expanded analysis. Selection rules and phase-matching conditions are found that govern the power transfer; these are shown to allow wave power to increase quadratically with both the interaction length and the dc beam current. Examples of fifth-harmonic conversion are presented for both TE_{32} and TE_{03} modes, the latter in a square waveguide supporting a circularly polarized wave. Power levels of 100 kW or more at 94 GHz appear to be achievable in a conceptual fifth-harmonic device using a 200-kV, 1-A beam. The circularly polarized mode appears to be relatively free of mode competition. Devices with lower beam energies are also shown to be capable of fifth-harmonic operation at 94 GHz, albeit with lower output power than for devices with higher beam energies.

PACS number(s): 41.60.Ap, 52.75.Ms, 41.75.Ht

I. INTRODUCTION

In a recent paper [1] (hereafter labeled I) the flow of power from a spatiotemporally modulated electron beam to the fields of a TE_{0m} mode in a rectangular waveguide was determined. The beam, which was assumed to have been prepared by cyclotron autoresonance acceleration [2], propagated along a uniform or weakly tapered axisymmetric static magnetic field B. The electron orbits in the beam were taken to be identical axis-encircling helical trajectories characterized by the phase variable $\phi_0+\xi z-pt$, where ϕ_0 is the initial phase value, ξ is the orbit pitch number, z is the axial coordinate, p is the temporal radian frequency, and t is the time. For such a beam equilibrium, the space and time variations are coupled (thus the choice of the modifier "spatiotemporal") with an effective phase velocity $c\beta_z/(1-\Omega/p)$, where $c\beta_z$ is the beam electrons' axial velocity, c is the speed of light, and $\Omega=eB/m\gamma$ is the gyration frequency for an electron of charge $-e$, mass m, and relativistic energy factor γ. When this effective phase velocity matches the phase velocity of a waveguide mode, it was shown in I that energy flow from the beam to the wave can be cumulative, increasing with the square of both the interaction distance and the dc beam current. Since the effective phase velocity can be adjusted to be either fast or slow, with respect to the speed of light, and either positive or negative, it is apparent that beam coupling to co- or counter-propagating waveguide modes is possible.

The results of I confirmed earlier research [3,4] in which it was shown that strong temporal modulation on a beam can allow efficient production of power at a harmonic of the modulation frequency when the beam interacts with a resonant cavity. But prior to I, it did not seem to have been recognized that the traveling-wave character of the spatiotemporally modulated beam allowed direct coupling to traveling guided electromagnetic waves as well. Of course, in the multicavity klystron [5] and the more recent gyroklystron [6] spatiotemporal modulation on the beam is imparted at the first cavity, enhanced in the intermediate cavities, and converted to radiation at the output cavity. And indeed the location of the gaps in these cavities is critical to the operation of the device. Perhaps the interaction described in Ref. [7] is that which most closely resembles what was described in I, although there the modulation and demodulation of the beam are weaker than what occurs in the interaction described in I.

The conversion of beam power to radiation in the traveling-wave interaction described in I is not due to a convective instability, which in an interaction calculated to *second-order* in the wave electric field would give rise to growth exponential in the interaction distance. Rather, the power transfer to the wave comes from the *first-order* generation of an electric field that is synchronous with the spatiotemporally modulated beam current driving the characteristic impedance of the waveguide. Power transfer remains cumulative as long as the effective wave on the beam and the electromagnetic wave remain in phase. In the nonlinear regime, this requires that the static magnetic field be tapered down, so as to maintain constant the aforementioned effective phase velocity as β_z and γ decrease. Since the particles can be kept in phase with one another along the downward-taper, it was speculated in I that the interaction could in principal convert 100% of the transverse energy on the beam into coherent radiation. This speculation has been confirmed in a preliminary way by numerical interaction of the governing equations [8], and is currently the subject of a particle simulation study [9].

The present paper extends I to include TE_{lm} modes of a rectangular waveguide. The method of solution mimics I in principal, but a number of complications not encountered in I arise due mainly to the inclusion of non-axis-encircling orbits and to the coupling with two transverse spatial dimensions in the dynamics. The restricted analysis in I is not competent to treat circularly polarized modes in square waveguides or interactions involving competing TE modes; both topics are explored in this paper. Under conditions of perfect phase matching between the beam and the traveling wave, the form of the power transfer found in the present paper, and that found in I, are nearly identical, subject to a set of selection rules derived for systems with some degree of symmetry that govern the magnitude of the coupling.

This paper undertakes to illustrate mode competition using two examples, where for illustration fifth-harmonic conversion to 94-GHz radiation is considered. One example employs a TE_{32}-mode rectangular waveguide, the second employs a TE_{03}-mode square waveguide, the latter supporting a circularly polarized wave. Both examples employ a 200-kV, 1-A beam, with a transverse-to-axial momentum ratio of 4. It is shown that mode competition, particularly for modes excited at the fourth and sixth temporal harmonics, is serious for the TE_{32} case, but is probably not an issue for the TE_{03} case. This is because the TE-mode spectrum is only half as dense for a square waveguide as for a rectangular waveguide, and because any potentially competing mode can be excited far from its cutoff frequency. As a result, it appears that an efficient 100-kW fifth-harmonic converter at 94 GHz could be designed based on the results of this paper. In addition, operation at beam energies down to 50 kV is examined, to show how the coupling parameters scale as the beam parameters change, and to suggest that some applications may be served by a low-voltage fifth-harmonic converter.

This paper is organized as follows. Section II contains the derivation for the power transfer from the beam to the guided wave. In Sec. III the results are evaluated for axis-encircling beams exciting TE_{0m} modes in rectangular waveguides (III A), TE_{mm} modes in square waveguides (III B), TE_{lm} modes in rectangular waveguides (III C) and TE_{0m} circularly polarized modes in square waveguides (III D). For non-axis-encircling beams, TE_{mm} modes in square waveguide are discussed (III E). Section IV contains a discussion of imperfect phase matching, which is especially important when considering competing modes. The examples are given in Sec. V. A summarizing discussion and conclusions are given in Sec. VI. The Appendix gives the power transfer calculation for circularly polarized modes, to show the origin of several peculiarities in the results.

II. POWER TRANSFER INTO TE_{lm} WAVEGUIDE MODES

The calculation presented in this section follows the method developed in I, where power flow into TE_{0m} modes in a rectangular waveguide was derived. In this paper, the calculation is extended to linearly polarized TE_{lm} modes and to circularly polarized modes. This introduces some additional mathematical complexity, but allows additional physical features to emerge. We consider axis-encircling beams, which have electron orbit centers of gyration on the waveguide center line, as well as non-axis-encircling beams. Selection rules are developed to identify the conditions under which power transfer from the beam to the wave is absent at either even or odd temporal harmonics of the fundamental modulation frequency on the beam. The formalism also provides prescriptions for selecting waveguide dimensions and for positioning the beam axis with respect to the waveguide axis to minimize coupling to one or more competing modes. It is found that power transfer rates as great as twice those for TE_{0m} modes can exist for TE_{lm} modes, since two polarizations of the field are able to couple to the beam, rather than one. When circularly polarized TE_{0m} modes are considered, power transfer rates twice those for linear polarization are also shown to be possible.

Following I, we consider a cold-electron beam with imposed spatiotemporal modulation passing along a uniform z-directed static magnetic field B. The transverse current density carried by the beam has components

$$\left.\begin{matrix} J_{0x}(x,y,z,t) \\ J_{0y}(x,y,z,t) \end{matrix}\right\} = -\frac{N_0 e W A}{\gamma}\delta(x-x_0-R\cos\phi) \tag{1}$$

$$\times\delta(y-y_0-R\sin\phi)\times\begin{cases} -\sin\phi \\ \cos\phi \end{cases}, \tag{2}$$

where $N_0 e$ is the charge concentration; A is the beam cross-sectional area; W and U are components of the beam electrons' momentum per unit rest mass across and along B; γ is the Lorentz energy factor, related to W and U by $\gamma^2c^2=c^2+W^2+U^2$; ϕ is the gyration phase of the helical orbits given by $\phi(z,t)=\phi_0+\xi z-pt$, with p the fundamental modulation frequency and $\xi=\gamma(p-\Omega)/U$ the fundamental orbit pitch number, both imposed on the beam during its formation such as in a cyclotron autoresonance accelerator [2], and with ϕ_0 the relative phase at $\xi z=pt$; $\Omega=eB/m\gamma$ is the relativistic electron gyrofrequency; $R=W/\gamma\Omega$ is the electron gyration radius; and x_0 and y_0 are the coordinates of the center of gyration.

We seek an expression for the power transfer from such a beam to the fields of a TE_{lm} rectangular waveguide, namely

$$E_x(x,y,z,t)=E_0(z)\sin\alpha\cos(k_x x)\sin(k_y y)\sin\theta(z,t) \tag{3}$$

and

$$E_y(x,y,z,t)=-E_0(z)\cos\alpha\sin(k_x x)\times\cos(k_y y)\sin\theta(z,t), \tag{4}$$

where $\tan\alpha=k_y/k_x$, $\theta(z,t)=k_\parallel z-\omega t$, $k_\perp^2=k_x^2+k_y^2$, and $(k_\perp^2+k_\parallel^2)c^2=\omega^2$. The line $(x=0,y=0,z)$ is along the lower left-hand corner of the waveguide; $k_x=l\pi/a$ and $k_y=m\pi/b$, where a and b are the width and height of the waveguide. The field amplitude $E_0(z)$ is assumed to be slowly varying with z, such that $k_\parallel^{-1}d[\ln E_0(z)]/dz \ll 1$.

The waveguide transverse magnetic-field components are given by $H_x(x,y,z,t)=-E_y(x,y,z,t)/Z_{\rm TE}$, and $H_y(x,y,z,t)=E_x(x,y,z,t)/Z_{\rm TE}$, where $Z_{\rm TE}=\eta(1-k_\perp^2c^2/\omega^2)^{-1/2}$ is the wave impedance with $\eta=(\mu_0/\epsilon_0)^{1/2}=120\pi$ Ω. The instantaneous power flow is

$$\begin{aligned}P(z,t)&=\int_0^a dx\int_0^b dy(E_xH_y-E_yH_x)\\&=Z_{\rm TE}^{-1}\int_0^a dx\int_0^b dy(E_x^2+E_y^2)\\&=abE_0^2(z)\sin^2\theta/2\epsilon_{l,m}Z_{\rm TE}\ ,\end{aligned}\tag{5}$$

where $\epsilon_{l,m}$ is the Neumann symbol, equal to 1 for either $l=0$ or $m=0$, and otherwise equal to 2. The time-averaged power flow is $P(z)=abE_0^2(z)/4\epsilon_{l,m}Z_{\rm TE}$. From Eq. (5), keeping only terms with a nonzero time average, we find

$$\frac{dP(z,t)}{dz}=abE_0(z)\left[\frac{dE_0(z)}{dz}\right]\sin^2\theta/\epsilon_{l,m}Z_{\rm TE}\ .\tag{6}$$

The beam currents give rise to growth in power flow along the waveguide according to the equation

$$\begin{aligned}\frac{dP(z,t)}{dz}&=-\int_0^a dx\int_0^b dy(J_{0x}E_x+J_{0y}E_y)\\&=\frac{N_0eWA}{\gamma}E_0(z)\sin\theta\Big\{-\sin\phi\cos(k_xx_0+k_xR\cos\phi)\sin(k_yy_0+k_yR\sin\phi)\sin\alpha\\&\qquad-\cos\phi\sin(k_xx_0+k_xR\cos\phi)\cos(k_yy_0+k_yR\sin\phi)\cos\alpha\Big\}\ .\end{aligned}\tag{7}$$

After manipulating Eq. (7) somewhat and after averaging over the time of interaction, we will equate Eqs. (6) and (7), to find an integrable expression for $dE_0(z)/dz$.

To simplify Eq. (7), we introduce the quantities r_0 and r_0^*, defined by

$$k_\perp r_0=k_xx_0+k_yy_0\ ,\quad k_\perp r_0^*=k_xx_0-k_yy_0\ .$$

This allows Eq. (7) to be written as

$$\frac{dP(z,t)}{dz}=-\frac{W}{2U}I_0E_0(z)\sin\theta\Big\{\cos(\phi-\alpha)\sin[k_\perp r_0+k_\perp R\cos(\phi-\alpha)]+\cos(\phi+\alpha)\sin[k_\perp r_0^*+k_\perp R\cos(\phi+\alpha)]\Big\}\ ,\tag{8}$$

where $I_0=N_0eAU/\gamma$ is the dc beam current. We now invoke the identity

$$\exp(ib\cos\zeta)=\sum_{n=0}^{\infty}(-1)^n[\epsilon_nJ_{2n}(b)\cos2n\zeta+2iJ_{2n+1}(b)\cos(2n+1)\zeta]\ ,$$

where $J_s(b)$ is the sth-order Bessel function of the first kind, and ϵ_n is again the Neumann symbol, equal to 1 for $n=0$ and otherwise equal to 2. After some manipulation involving use of a Bessel function recursion relation, Eq. (8) can be written in turn as

$$\begin{aligned}\frac{dP(z,t)}{dz}=-\frac{W}{U}I_0E_0(z)\sin\theta\sum_{n=0}^{\infty}(-1)^n\Big\{&K_{2n+1}(k_\perp R)[\sin(k_\perp r_0)\cos(2n+1)(\phi-\alpha)+\sin(k_\perp r_0^*)\cos(2n+1)(\phi+\alpha)]\\&-K_{2n}(k_\perp R)[\cos(k_\perp r_0)\cos2n(\phi-\alpha)+\cos(k_\perp r_0^*)\cos2n(\phi+\alpha)]\Big\}\ ,\end{aligned}\tag{9}$$

where $K_s(b)=(\epsilon_s/2)[dJ_s(b)/db]$. Equation (9) can now be equated to Eq. (6), to yield

$$\sin^2\theta\frac{dE_0(z)}{dz}=-\frac{\epsilon_{l,m}Z_{\rm TE}}{ab}\frac{W}{U}I_0\sin\theta\sum_{n=0}^{\infty}(-1)^n\mathcal{T}_n\ ,\tag{10}$$

where $\mathcal{T}_n$ represents the term in curly brackets in Eq. (9).

Next, a time average over the time of interaction $T=z\gamma/U$ is carried out. On the left-hand side of Eq. (10) a factor $\frac{1}{2}$ results for the time average of $\sin^2\theta$, since $\omega T\gg1$. On the right-hand side we require the integrals

$$\begin{aligned}g_s^{(\pm)}(z)&=\frac{U}{z\gamma}\int_0^{z\gamma/U}dt\,\sin(k_\parallel z-\omega t)\cos[s(\phi_0\pm\alpha)+s(\xi z-pt)]\\&=-\frac{U}{2z\gamma(\omega-sp)}\Big\{\cos[s(\phi_0\pm\alpha)+(s\xi-k_\parallel)z]-\cos[s(\phi_0\pm\alpha)+(s\xi-k_\parallel)z+(\omega-sp)z\gamma/U]\Big\}\ ,\end{aligned}\tag{11}$$

in terms of which one obtains the time-averaged result

$$\frac{dE_0(z)}{dz}=-\frac{2\epsilon_{l,m}Z_{\mathrm{TE}}}{ab}\frac{W}{U}I_0\sum_{n=0}^{\infty}(-1)^n\left\{K_{2n+1}(k_\perp R)[g_{2n+1}^{(-)}(z)\sin(k_\perp r_0^*)+g_{2n+1}^{(+)}(z)\sin(k_\perp r_0^*)]\right.$$
$$\left.-K_{2n}(k_\perp R)[g_{2n}^{(-)}(z)\cos(k_\perp r_0^*)+g_{2n}^{(+)}(z)\cos(k_\perp r_0^*)]\right\}. \quad (12)$$

In deriving Eq. (12), a term containing $(\omega+sp)$ in place of $(\omega-sp)$ has been omitted, due to its small magnitude and rapidly varying temporal nature. Equation (12) may be integrated along the interaction length from $z=0$ to L, yielding for the amplitude of the sth-harmonic electric field the result

$$E_s(L)=E_s(0)+\frac{2\epsilon_{l,m}Z_{\mathrm{TE}}}{ab}\frac{W}{U}I_0K_s(k_\perp R)\times\begin{cases}S(L), & s \text{ odd}\\ C(L), & s \text{ even}\end{cases} \quad (13)$$

where

$$S(L)=(-1)^{(s+1)/2}[G_s^{(-)}(L)\sin(k_\perp r_0)+G_s^{(+)}(L)\sin(k_\perp r_0^*)] \quad (14)$$

and

$$C(L)=(-1)^{s/2}[G_s^{(-)}(L)\cos(k_\perp r_0)+G_s^{(+)}(L)\cos(k_\perp r_0^*)], \quad (15)$$

with $G_s^{(\pm)}(L)=\int_0^L dz\, g_s^{(\pm)}(z)$, and $E_s(0)$ the input field. The quantities $S(L)$ and $C(L)$ are geometric factors that govern the coupling of power to the waveguide fields at either odd or even temporal harmonics of the beam modulation frequency p, respectively. Hereafter, these shall be referred to as the geometric coupling factors. We shall develop selection rules from these factors for symmetric systems that govern the growth of radiation into a given waveguide mode at a given temporal harmonic.

The cumulative power flow at the sth harmonic follows from Eq. (13) as $P_s(L)=abE_s^2(L)/4\epsilon_{l,m}Z_{\mathrm{TE}}$. Cross terms with different s values do not contribute, since these would involve products of different harmonic functions of p which have zero time average.

III. EVALUATION OF THE POWER TRANSFER

As was discussed in I, the integrals $G_s^{(\pm)}(L)$ will tend towards zero as L increases, unless both $(\omega-mp)$ and $(k_\parallel-m\xi)$ are themselves zero. This amounts to a requirement for spatiotemporal phase matching over the length and time of the interaction, without which phase interference will prevent cumulative power transfer from the beam to the wave. The phase difference ϕ_0 between the beam current and the field will automatically adjust itself to maximize the power transfer to the field. However, the value of this phase difference will depend upon the two coefficients, as well as upon the two integrals $G_s^{(\pm)}(L)$ in Eqs. (14) and (15). To illustrate, we choose the simple case with $\alpha=0$, and $\sin k_\perp r_0=\sin k_\perp r_0^*=1$. We now have $C(L)=0$, and

$$|S(L)|=L|\sin(s\phi_0)I_1(\theta_1,\theta_2)-\cos(s\phi_0)I_2(\theta_1,\theta_2)|, \quad (16)$$

where

$$I_1(\theta_1,\theta_2)=\frac{1}{\theta_2}\int_{\theta_1}^{\theta_1+\theta_2}du\frac{\sin u}{u}=\frac{1}{\theta_2}[\mathrm{Si}(\theta_1+\theta_2)-\mathrm{Si}(\theta_1)]$$

and

$$I_2(\theta_1,\theta_2)=\frac{1}{\theta_2}\int_{\theta_1}^{\theta_1+\theta_2}du\frac{(\cos u-1)}{u}=\frac{1}{\theta_2}[\mathrm{Ci}(\theta_1+\theta_2)-\mathrm{Ci}(\theta_1)-\ln(1+\theta_2/\theta_1)]$$

with $\theta_1=(s\xi-k_\parallel)L$, $\theta_2=(\omega-sp)\gamma L/U$, and $\mathrm{Si}(x)$ and $\mathrm{Ci}(x)$ are the sine-integral and cosine-integral functions [10]. Differentiating Eq. (16) with respect to $s\phi_0$ to find the value which maximizes $|S(L)|$ gives

$$\tan(s\phi_0)=-I_1(\theta_1,\theta_2)/I_2(\theta_1,\theta_2)$$

and

$$\max S^2(L)=L^2[I_1^2(\theta_1,\theta_2)+I_2^2(\theta_1,\theta_2)].$$

Figure 1 depicts $\max S^2(L)/L^2$ as a function of θ_1 and θ_2. As can be seen, the function has a peak value of unity at $\theta_1=\theta_2=0$, has local maxima along $\theta_1=-\theta_2=\theta$, and falls below 0.113 for $\theta>10$.

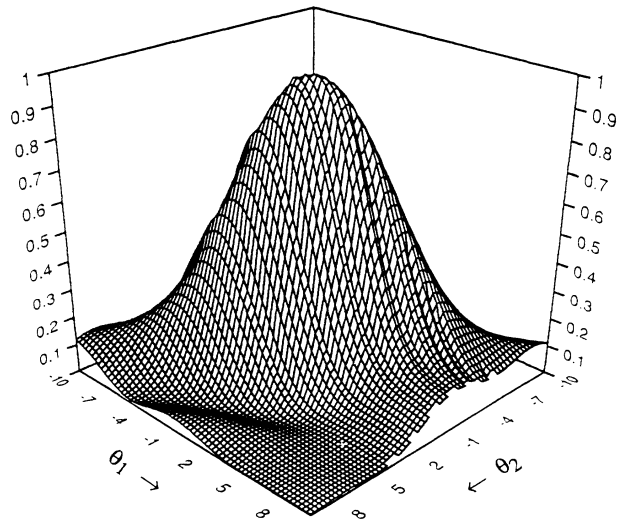

FIG. 1. Diminution of power transfer from beam to wave due to imperfect phase matching for $\alpha=0$. See text for definitions of parameters.

We shall discuss specific examples of imperfect phase-matching below but, in the remainder of this section, we shall assume that the two matching conditions are fulfilled, i.e., $\theta_1=\theta_2=0$, in which case we have

$$G_s^{(\pm)}(L)=-\frac{L}{2}\sin(s\phi_0\pm s\alpha)\ . \tag{17}$$

This allows the geometric coupling factors Eqs. (14) and (15) to be written as follows:

$$|S(L)|=L\,|\sin(s\phi_0)\cos(s\alpha)\sin(k_x x_0)\cos(k_y y_0) -\cos(s\phi_0)\sin(s\alpha)\cos(k_x x_0)\sin(k_y k_0)| \tag{18}$$

and

$$|C(L)|=L\,|\sin(s\phi_0)os(s\alpha)\cos(k_x x_0)\cos(k_y y_0) +\cos(s\phi_0)\sin(s\alpha)\sin(k_x x_0)\sin(k_y y_0)|\ . \tag{19}$$

We now consider special cases.

A. TE_{0m} modes, axis-encircling beam

First, we consider the case treated in I for TE_{0m} waveguide modes with an axis-encircling beam by taking $k_x=0$, $k_y=m\pi/b$, and $y_0=b/2$. Thus $\alpha=\pi/2$ and $k_y y_0=m\pi/2$. As a result, we find from Eqs. (18) and (19)

$$|S(L)=\begin{cases}0\ , & s \text{ even or } m \text{ even}\\ L\,|\cos(s\phi_0)|\ , & s \text{ odd and } m \text{ odd}\end{cases} \tag{20}$$

and

$$|C(L)|=\begin{cases}0\ , & s \text{ odd or } m \text{ odd}\\ L\,|\sin(s\phi_0)|\ , & s \text{ even and } m \text{ even}\ .\end{cases} \tag{21}$$

This shows that odd and even temporal harmonics are selectively coupled respectively to wave guide modes with even (m odd) and odd (m even) spatial symmetry. This selectivity is of importance in combating spatial mode competition, since it cuts in half the number of waveguide modes that can, in principle, couple to the beam, and thus increases the mismatch in phase for the nearest competing modes to more than would be the case without this selectivity.

In either the case of even or odd temporal harmonics, the form of the result for power transfer found in I is recovered, namely

$$P(L)=P(0)+\frac{W}{U}I_0E_0(0)LK_s(k_\perp R) +\frac{\epsilon_{l,m}Z_{\mathrm{TE}}}{ab}\left[\frac{W}{U}I_0LK_s(k_\perp R)\right]^2\ , \tag{22}$$

since the relative phase ϕ_0 between the fields and the beam gyrations will adjust itself in each case so that either $|S(L)|=L$ or $|C(L)|=L$ [11]. For TE_{0m} modes $\epsilon_{l,m}=1$. As was pointed out in I, Eq. (22) indicates that power transfer occurs even when $E_0(0)$ is zero, i.e., even when there is no input signal. The power grows quadratically with the interaction length and the beam current. Examples of devices to generate power at 94 and 1000 GHz are given in I.

B. TE_{mm} modes in square waveguide, axis-encircling beam

We next consider an axis-encircling beam coupling in a square waveguide to TE_{mm} modes. Here $k_x x_0=k_y y_0=m\pi/2$, and $\alpha=\pi/4$. For this case, we find from Eqs. (18) and (19)

$$|C(L)|=L\,|\sin(s\phi_0)\cos(s\pi/4)\cos^2(m\pi/2) +\cos(s\phi_0)\sin(s\pi/4)\sin^2(m\pi/2)| \tag{23}$$

and

$$|S(L)|=L\,|\sin(s\phi_0)\cos(s\pi/4)-\cos(s\phi_0)\sin(s\pi/4)| \times|\cos(m\pi/2)\sin(m\pi/2)|=0\ . \tag{24}$$

Since $S(L)=0$ for all m, one sees that radiation only at even values of s (i.e., even temporal harmonics) is coupled out in this case. Equation (23) gives $|C(L)|=L\,|\sin(s\phi_0)|$ for even m when $s=4,8,12,\ldots,4n$, while $|C(L)|=L\,|\cos(s\phi_0)|$ for odd m when $s=2,6,10,\ldots,(4n-2),\ldots$; otherwise $|C(L)|=0$. The magnitude of the power transfer is given by Eq. (22) in this case, subject to the above selection rules, but since here $\epsilon_{l,m}=2$, it is seen that the third term in Eq. (22) is twice what it is for TE_{0m} modes. With two field components available to couple to the beam, twice the power can be transferred under otherwise equal conditions, as compared to modes with only one field component.

C. TE_{lm} modes in rectangular waveguide, axis-encircling beam

In this case, $k_x x_0=l\pi/2$, $k_y y_0=m\pi/2$, and $\tan\alpha=ma/lb$. The geometric coupling factors are, from Eqs. (18) and (19),

$$|S(L)|=L\,|\sin(s\phi_0)\cos(s\alpha)\sin(l\pi/2)\cos(m\pi/2) -\cos(s\phi_0)\sin(s\alpha)\cos(l\pi/2)\sin(m\pi/2)| \tag{25}$$

and

$$|C(L)|=L|\sin(s\phi_0)\cos(s\alpha)\cos(l\pi/2)\cos(m\pi/2) +\cos(s\phi_0)\sin(s\alpha)\sin(l\pi/2)\sin(m\pi/2)|\ . \tag{26}$$

If l and m are either both even or both odd, Eq. (25) shows that $S(L)=0$, so that only even harmonics of p are coupled from the beam. Similarly, if one index is even and the other odd, Eq. (26) shows that $C(L)=0$, so that only odd harmonics of p are coupled from the beam. In particular, the geometric coupling factors are as follows:

$$|C(L)|=L\,|\sin(s\phi_0)\cos(s\alpha)|,\quad l \text{ even},\ m \text{ even}; \tag{27}$$

$$|C(L)|=L\,|\cos(s\phi_0)\sin(s\alpha)|,\quad l \text{ odd},\ m \text{ odd}; \tag{28}$$

$$|S(L)|=L\,|\sin(s\phi_0)\cos(s\alpha)|,\quad l \text{ odd},\ m \text{ even}; \tag{29}$$

and

$$|S(L)|=L\,|\cos(s\phi_0)\sin(s\alpha)|,\quad l \text{ even},\ m \text{ odd}. \tag{30}$$

These equations show that, in general, the magnitudes of the geometric coupling factors will be less than L, since the values of $\cos(s\alpha)$ and $\sin(s\alpha)$ will be less than

unity. However, by a judicious choice of the waveguide dimensions, one of these can be unity for a particular waveguide mode, and less than unity for a nearby completing mode. An example of this is given in Sec. IV.

D. Circularly polarized waveguide modes, axis-encircling beam

It might be expected that stronger wave growth than that described in the preceding sections of this paper might be possible if the waveguide can support circularly polarized modes. In a rectangular waveguide, circular polarization arises from a superposition of two modes with the same phase velocity such that the field pattern rotates $\pi/2$ without change in amplitude or spatial pattern each temporal quarter cycle. The only superposition that can satisfy this is a TE_{0m} and a TE_{m0} mode of equal amplitudes in a square waveguide, provided one propagates as $\sin\theta(z,t)$ while the second propagates as $\sigma\cos\theta(z,t)$. The parameter σ takes on values of ± 1, and allows consideration of either a clockwise $(+1)$ or counterclockwise (-1) sense of rotation. Thus the waveguide electric field we consider is

$$\mathbf{E}(x,y,z,t)=E_0(z)[\hat{\mathbf{e}}_x\sin(k_m y)\sin\theta + \hat{\mathbf{e}}_y\sigma\sin(k_m x)\cos\theta] , \tag{31}$$

where $k_m=m\pi/a$ and $\theta(z,t)=k_{\parallel}z-\omega t$.

The derivation for the power transfer from a beam with current density given by Eqs. (1) and (2) to this waveguide field follows the same procedure as was followed in Sec. II. An outline of the derivation is given in the Appendix. The results are summarized here.

For waveguide modes with even spatial symmetry (m odd) we find that only odd temporal harmonics are excited. The field amplitude obeys

$$\frac{dE_0(z)}{dz}=2I_0\frac{W}{U}\frac{Z_{\mathrm{TE}}}{a^2}(-1)^{(m-1)/2} \times\sum_{n=0}^{\infty}K_{2n+1}(k_m R)\sin[\theta+\sigma(-1)^n(2n+1)\phi] . \tag{32}$$

Likewise, for waveguide modes with odd spatial symmetry (m even) we find that only even temporal harmonics are excited. The field amplitude obeys

$$\frac{dE_0(z)}{dz}=2\sqrt{2}I_0\frac{W}{U}\frac{Z_{\mathrm{TE}}}{a^2}(-1)^{m/2} \times\sum_{n=0}^{\infty}K_{2n}(k_m R)\sin 2n\phi \times\sin[\theta+\sigma(-1)^{n-1}\frac{\pi}{4}] . \tag{33}$$

Integration over the interaction time and the interaction length, as in Sec. II, yields for $\omega=sp$, $k_{\parallel}=s\xi$, and $E_0(0)=0$,

$$P_s(L)=\begin{cases} 2Z_{\mathrm{TE}}\left[\frac{L}{a}\right]^2 I_0^2\left[\frac{W}{U}\right]^2 K_s^2(k_m R) \\ \quad \text{for } m \text{ odd, } s \text{ odd} \qquad (34) \\ Z_{\mathrm{TE}}\left[\frac{L}{a}\right]^2 I_0^2\left[\frac{W}{U}\right]^2 K_s^2(k_m R) \\ \quad \text{for } m \text{ even, } s \text{ even.} \qquad (35) \end{cases}$$

The result for odd temporal harmonics [Eq. (34)] is seen to be twice that for linear polarization [see Eq. (22)] and twice that for even temporal harmonics [Eq. (35)]. However, the result given by Eq. (34) is subject to the following selection rules for the sense of circular polarization of the wave that can satisfy frequency and wave number matching with the beam:

$$s=\begin{cases} 1,5,9,13,\ldots,(4n+1),\ldots, \\ \sigma=+1 \text{ (counterclockwise rotation)} \\ 3,7,11,15,\ldots,(4n-1),\ldots, \\ \sigma=-1 \text{ (clockwise rotation).} \end{cases}$$

Of course, the wave will automatically emerge in that polarization for which the power transfer is greatest, just as the relative phase ϕ_0 will adjust itself to maximize the power transfer. But in utilizing the power generated, it could be important to have knowledge of the polarization, which has been shown here not to conform to simple intuition.

E. TE_{mm} mode in square waveguide, non-axis-encircling beam

As an example of coupling to a non-axis-encircling beam, we consider a beam centered along the waveguide diagonal with $x_0=y_0=R_0/\sqrt{2}$ so that $\alpha=\pi/4$. Equations (18) and (19) can then be written

$$S(L)=\frac{L}{2}|\sin(k_\perp R_0)\sin(s\phi_0-s\pi/4)| \tag{36}$$

and

$$|C(L)|=L|\sin(s\phi_0)\cos(s\pi/4)\cos^2(k_\perp R_0/2) +\cos(s\phi_0)\sin(s\pi/4)\sin^2(k_\perp R_0/2)| , \tag{37}$$

where $k_\perp=\sqrt{2}k_m$. Thus, either even or odd temporal harmonics can be excited, in contrast to the case of square waveguide with an axis-encircling beam, where only even temporal harmonics are excited. But for example, when the beam axis is located so that $k_\perp R_0=n\pi$, where n is an integer, the geometric coupling factors become

$$|S(L)|=0 \tag{38}$$

and

$$|C(L)|=\begin{cases} L\,|\cos(s\phi_0)\sin(s\pi/4)|, & n \text{ odd} \quad (39)\\ L\,|\sin(s\phi_0)\cos(s\pi/4)|, & n \text{ even} . \quad (40)\end{cases}$$

Thus, for n even $|C(L)|=0$ for $s=2,6,10,\ldots,(4j+2),\ldots$, while for n odd $|C(L)|=0$ for $s=4,8,12,\ldots,(4j),\ldots$. As a result, coupling to every other even harmonic and to all odd harmonics may be suppressed by this judicious choice of the beam axis. For instance, with $m=10$ and $x_0/a=\frac{9}{20}$, a device designed to operate at the tenth harmonic would not have coupling in the $TE_{10,10}$ mode at any neighboring harmonics closer that the sixth or the fourteenth. But since the design cutoff frequency would be slightly below the tenth-harmonic frequency, the sixth harmonic would be cutoff and the fourteenth harmonic would have much lower initial wave growth than the tenth, as well as a large mismatch in phase velocity with the beam's spatiotemporal modulation. Similar geometric considerations apply for rectangular wave guides with non-axis-encircling beams that permit a variety of mode-suppression strategies to be employed.

IV. IMPERFECT PHASE MATCHING

In this section, we attempt to assess the potential for minimizing wave growth at a given frequency in waveguide modes other than the design mode. Such mode competition can reduce the output power of a harmonic converter based on the principles discussed in this paper since waves of differing phase velocity can interfere destructively and significantly reduce the transfer of power to the waves. To find the growth rates of competing modes, it is necessary to evaluate the integrals $G_s^{(\pm)}(L)$ and their influence upon the geometric coupling factors $S(L)$ and $C(L)$ as given by Eqs. (14) and (15). Figure 1 shows graphically the effect upon coupling of a mismatch in both frequency or wave number. However, we can obtain an analytical form for $G_s^{(\pm)}(L)$ when frequency matching prevails, but wave-number matching does not.

From Eq. (11), in the limits as $\omega\rightarrow sp$, we find

$$g_s^{(\pm)}(z)=-\tfrac{1}{2}\sin[s(\phi_0\pm\alpha)+(s\xi-k_\parallel)z] . \quad (41)$$

Thus $G_s^{(\pm)}(L)=\int_0^L dz\, g_s^{(\pm)}(z)$ follows as

$$G_s^{(\pm)}(L)=\frac{1}{2(s\xi-k_\parallel)}\left\{\cos[s(\phi_0\pm\alpha)+(s\xi-k_\parallel)L]-\cos[s(\phi_0\pm\alpha)]\right\} . \quad (42)$$

We shall now assume, for simplicity, that the beam axis is positioned such that only one term in either Eq. (14) or (15) is nonzero. This enables the relative phase ϕ_0 for maximum power transfer to be easily determined, much as was done to find Eq. (16). This gives the value of $s(\phi_0\pm\alpha)$ which maximizes $G_x^{(\pm)}(L)$ to be

$$s(\phi_0\pm\alpha)=\cot^{-1}[\csc(s\xi-k_\parallel)L-\cot(s\xi-k_\parallel)] . \quad (43)$$

This leads to the maximum value of $G_s^{(\pm)}(L)$ as follows:

$$\max|G_s^{(\pm)}(L)|=\frac{L}{2}\frac{\sin[(s\xi-k_\parallel)L/2]}{[(s\xi-k_\parallel)L/2]} . \quad (44)$$

We shall use this last expression to evaluate the wave growth for modes other than the design mode by substituting $k_\parallel=s\xi$ for the design mode and $k_\parallel=k_\parallel'$ for the competing mode.

V. EXAMPLES

In this section, we give two illustrative examples of parameters for devices to generate radiation at 94 GHz. In I two examples at the fifth harmonic from beams modulated at 18.8 GHz were given, one using a 300-kV beam in a TE_{30} rectangular waveguide and a second using a 500-kV beam in a TE_{50} waveguide [11]. The examples given in this section will be based on use of a 200-kV beam which, as will be shown, can provide ample power growth at the fifth harmonic of the beam rotation frequency p. The first illustrative device utilizes an axis-encircling beam in a rectangular waveguide supporting a TE_{32} mode, while the second utilizes an axis-encircling beam in a square waveguide supporting a circularly polarized TE_{30} mode. For both cases we will evaluate growth rates for competing waveguide modes at the fifth harmonic as well as other competing harmonics. These examples show that operation in a square waveguide allows suppression of mode competition that is shown to seriously impede single-mode interaction in a rectangular waveguide. Operation of fifth-harmonic devices at beam energies lower than 200 kV will also be discussed briefly.

A. TE_{32} rectangular waveguide

The TE_{32} rectangular waveguide mode is chosen for a fifth-harmonic example since the selection rules of Sec. III C dictate that one mode index must be even and the other odd; otherwise coupling is absent. Furthermore, as shall be seen, the waveguide dimensions will accommodate the axis-encircling beam.

Equation (29) states that maximum coupling to this mode will result if $|\cos(5\alpha)|=1$, so that the allowed values of α include $\pi/5$, $2\pi/5$, etc. Therefore one has $ma/lb=\tan\alpha=0.7265$, 3.0777, etc. For $l=3$ and $m=2$, this gives $a/b=1.0898$, 4.6165, etc.

To proceed further, we must apply the conditions for phase matching between the beam and the wave. These conditions, which were derived in I, are

$$k_\parallel c=\omega\beta_\parallel \quad (45)$$

and

$$k_\perp R=s\left[\frac{\gamma^2\beta_\perp^2}{1+\gamma^2\beta_\perp^2}\right]^{1/2} , \quad (46)$$

where $\beta_\parallel=U/c\gamma$ and $\beta_\perp=W/c\gamma$. For a 200-kV beam with $W/U=4$, Eq. (45) gives $k_\parallel=3.3201\ \text{cm}^{-1}$ at 94 GHz, while Eq. (46) gives $k_\perp R=3.4218$. The magnetic-field value, as derived in I, is given by $\Omega/p=1-\beta_\parallel^2=0.9716$. Since here $p=(2\pi)18.8$ GHz, this

TABLE I. Power transfer at 94 GHz to TE modes that can compete with the design mode TE_{32}. Waveguide dimensions are 0.600×0.551 cm^2. Axis-encircling 200-kV beam has a velocity ratio $W/U=4.0$. Listed are the respective cutoff frequencies f_c, axial wave numbers $k_\parallel$, relevant coupling parameters $|\sin5\alpha|$ or $|\cos5\alpha|$ and $k_\perp R$, fifth-harmonic coupling constants $K_5(k_\perp R)$, initial power growth rates $P(L)/(I_0L)^2$ which do not include wave-number mismatch, and power transfers $P(L)/I_0^2$ after an interaction length of 8.0 cm, including phase interference effects. (Figures in brackets are power of 10.)

Mode	f_c (GHz)	$k_\parallel$ (cm^{-1})	$\lvert\sin5\alpha\rvert$ or $\lvert\cos5\alpha\rvert$	$k_\perp R$	$K_5(k_\perp R)$	$P(L)/(I_0L)^2$ (W/A^{2}cm^2)	$P(L=8.0\text{ cm})/I_0^2$ (W/A^2)
TE_{10}	24.986	18.979	1.000	0.923	9.53[−4]	3.38[−2]	2.09[−5]
TE_{01}	27.231	18.843	1.000	1.006	1.23[−3]	5.78[−2]	4.36[−4]
TE_{21}	56.910	15.669	0.603	2.102	1.97[−2]	1.78[+1]	2.73[−2]
TE_{12}	59.919	15.169	0.837	2.213	2.33[−2]	2.57[+1]	5.29[−2]
TE_{30}	74.959	11.880	1.000	2.768	4.78[−2]	1.38[+2]	7.34[−1]
TE_{03}	81.692	9.740	1.000	3.017	6.13[−2]	2.77[+2]	7.28
TE_{32}	92.654	3.320	1.000	3.422	8.49[−2]	1.56[+3]	1.00[+5]

gives $B=9.0728$ kG, so that $R=c\beta_\perp/\Omega=0.1763$ cm and $k_\perp=19.405$ cm^{-1}. The harmonic coupling constant $K_5(k_\perp R)=J_5'(k_\perp R)=0.08493$.

The waveguide dimensions are determined from $a=(\pi l/k_\perp)[1+(ma/lb)^2]^{1/2}$. For $(a/b)=1.0898$ and 4.6165 one finds $a=0.6003$ and 1.5717 cm, and $b=0.5509$ and 0.3405 cm, respectively. Only the first set of waveguide dimensions will accommodate an axis-encircling beam with a gyration radius of 0.1763 cm, so it is the obvious choice.

We evaluate the third term in Eq. (22), using $Z_{TE}=120\pi/\beta_\parallel$ from Eq. (45), to find $P(L)=1562(I_0L)^2$ W, for I_0 in A and L in cm, corresponding to an output power of 100 kW for a 1-A beam at $L=8.0$ cm, assuming linear theory to still be valid at this power level, a point that is discussed in Sec. VI of this paper.

Coupling parameters and wave growth rates at the fifth harmonic have been calculated for other TE modes with cutoff frequencies below 94 GHz for the same waveguide dimensions and the same electron beam as in the above example. Only modes with one index even and the other odd are chosen in view of the selection rules Eqs. (29) and (30). (This reduces from 13 to 7 the number of modes that must be considered.) Results are shown in Table I. The initial growth rates $P(L)/(I_0L)^2$ are evaluated without including the phase interference factor $(\sin\theta/\theta)^2$ as given by Eq. (44), with $\theta=(k_\parallel-k_\parallel')L/2$ while the values of $P(L=8.0\text{ cm})/I_0^2$ include this factor. The competing modes of consequence are seen to be TE_{03} and TE_{30}, for which the initial growth rates are 18% and 8.9% that of the TE_{32} mode, respectively. However, after evolving a distance of 8.0 cm these modes are seen to grow to less than 10^{-4} times the power level of the TE_{32} mode. Of course, these results assume that the modes evolve independently according to the predictions of linear theory as derived in this paper. It is conceivable that nonlinear coupling between the modes at small interaction lengths could cause the final power level in the TE_{32} mode to differ somewhat from what is shown in Table I. It will be shown in the example of Sec. V B that choice of a square waveguide for supporting circularly polarized modes can help to suppress the competition from nearby modes because of the sparsity of the available mode spectrum.

It is also of interest to find the power levels generated for harmonics other than the design harmonic. For the example given above, where the design harmonic is the fifth, we can find the power flow into waveguide modes which will couple to other harmonics. Table II shows results of this for the modes with the highest linear growth rates for the harmonics indicated. It is apparent that without some form of filtering in the output waveguide, coupling at the fourth and sixth harmonics would interfere significantly with that at the fifth. This fact provides

TABLE II. Power transfer at various harmonics which can compete with the fifth harmonic, for the same beam and waveguide parameters as in Table I. For each harmonic, the waveguide mode with the highest growth rate has been selected. (Figures in brackets are powers of 10.)

Harmonic s	f (GHz)	Mode	f_c (GHz)	$\omega/k_\parallel c$	$k_\perp R$	$K_5(k_\perp R)$	$P(L)/(I_0L)^2$ W/A cm)^2	$P(L=8.0\text{ cm})/I_0^2$ (W/A^2)
3	56.40	TE_{01}	27.231	1.142	1.006	0.057	1.34[+2]	4.40[−1]
4	75.20	TE_{22}	73.914	5.435	2.730	0.115	2.53[+3]	5.54[+4]
5	94.00	TE_{32}	92.654	5.926	3.422	0.085	1.56[+3]	1.00[+5]
6	112.80	TE_{33}	110.870	5.425	4.094	0.063	7.26[+2]	1.90[+3]
7	131.60	TE_{43}	129.080	5.133	4.767	0.046	3.91[+2]	3.32[+2]

further motivation to examine the interaction with circularly polarized modes in a square waveguide where undesired harmonics can possibly be suppressed, again due to the sparse mode spectrum.

B. Circularly polarized TE_{03} mode

In the example discussed in Sec. V A, the initial power growth at the fifth harmonic is predominantly in the design mode TE_{32}, although the growth rates in at least two other modes are not insignificant. But after a growth length of 8.0 cm, power in the TE_{32} mode is predicted to grow to 100 kW, which is a factor of about 10^4 larger than that of the competing modes. This demonstrates the powerful effect of imperfect phase matching in preventing the cumulative flow of power in a waveguide mode not phase matched to the beam's spatiotemporal modulation. However, it is also demonstrated that the fastest growing modes at other harmonics are not strongly suppressed, since among the plethora of available modes at least one at each competing harmonic is not greatly mismatched in phase with the beam.

This competition from interactions at other harmonics could be alleviated by use of a waveguide circuit with high- and low-pass filters to block unwanted frequencies. A simpler alternative is to employ a square waveguide which, because of mode degeneracy, will have half the number of independent modes as a rectangular waveguide of the same cutoff frequency.

In the example of this to be described, we employ the same electron beam as in the example of Sec. V A, with a beam energy of 200 kV and a velocity ratio $W/U=4.0$. The beam is axis encircling. From the selection rules of Sec. III D, a mode with an odd mode index is required. As shall be seen, the TE_{03} mode is the lowest which can accommodate the axis-encircling beam. In addition, odd-harmonic excitations in circular polarization were shown to have twice the growth rate as do even-harmonic excitations. For the fifth harmonic, the sense of mode rotation is counterclockwise. (See Sec. III D.)

Following the procedure of Sec. V A allows one to determine the device parameters, which are shown in Table III. The power growth rate is somewhat higher in this case than in the TE_{32} rectangular waveguide example of Sec. V A because the waveguide cross-sectional area is smaller in the present instance. Linear theory predicts that the output power at 94 GHz would rise to 100 kW in an interaction length of 6.8 cm for a beam current of 1 A.

The only modes that can compete with the design mode at the fifth harmonic are the TE_{01}/TE_{10} and the TE_{12}/TE_{21} degenerate sets. For these the initial power growth rates are 0.239 and 105 $W/A^2\,cm^2$, the latter of which is only 4.8% that of the design mode. (In the above rectangular waveguide example a growth rate 18% that of the design mode was found for the strongest fifth-harmonic competitor.) After an interaction length of 6.8 cm, these competing modes have 10^{-4} the power of the design mode, or less.

At harmonics other than the fifth, the fastest growing mode sets are TE_{01}/TE_{10} (third harmonic), TE_{02}/TE_{20} (fourth harmonic), TE_{13}/TE_{31} (sixth harmonic), and TE_{14}/TE_{41} (seventh harmonic). The initial power growth rates for these are 307, 606, 175, and 414 $W/A^2\,cm^2$, respectively, as compared with 2170 $W/A^2\,cm^2$ for the fifth harmonic. These other harmonic growth rates are proportionally much lower than those found in the above rectangular waveguide example. After an interaction length of 6.8 cm, the other harmonics have evolved to only 153, 11.9, 3.05, and 5.14 W/A^2, respectively, as compared with 100 kW/A^2 for the fifth harmonic.

C. Interactions with beam energies below 200 kV

The example presented in Sec. V B employs a 200-kV beam with a velocity ratio $W/U=4.0$ interacting with a circularly polarized TE_{03} mode in a square waveguide. The linear power growth rate found is 2170 $W/(A\,cm)^2$. This would indicate that a power output of 100 kW, corresponding to a harmonic conversion efficiency of 50%, could be expected for a 1-A beam after an interaction length of 6.8 cm. The validity of the assumption that linear theory holds at 50% conversion efficiency is discussed in Sec. VI. However, in comparing the interactions which are possible at beam energies lower than 200 kV, we shall consider the interaction lengths $L_{50\%}$ required to achieve 50% harmonic conversion efficiency based on linear theory to be a valid measure of the relative strengths of the interaction.

Table IV gives the parameters and the power growth rates for beams with velocity ratios $W/U=4.0$ and beam

TABLE III. Power transfer into modes of a square waveguide of width $a=0.486$ cm from a 200-kV beam with $W/U=4.0$. The design mode is TE_{03} at 94 GHz ($s=5$) in circular polarization. The only competing modes at 94 GHz are TE_{01} and TE_{12}. Modes that grow most rapidly at the harmonics $s=3$, 4, 6, and 7 are also included for comparison. (Figures in brackets are powers of 10.)

Harmonic s	f (GHz)	Mode	f_c (GHz)	$\omega/k_\parallel c$	$k_\perp R$	$K_s(k_\perp R)$	$P(L)/(I_0L)^2$ W/(A cm)^2	$P(L=6.8\text{ cm})/I_0^2$ (W/A^2)
3	56.40	TE_{01}	30.884	1.195	1.141	7.08[−2]	3.07[+2]	1.53[+2]
4	75.20	TE_{02}	61.769	1.753	2.281	8.19[−2]	6.06[+2]	1.19[+1]
5	94.00	TE_{03}	92.653	5.930	3.422	8.49[−2]	2.17[+3]	1.00[+5]
5	94.00	TE_{01}	30.884	1.059	1.141	2.11[−3]	2.39[−1]	4.08[−3]
5	94.00	TE_{12}	69.059	1.474	2.550	3.72[−2]	1.05[+2]	7.52[−1]
6	112.80	TE_{13}	97.665	2.000	3.607	4.11[−2]	1.75[+2]	3.05
7	131.60	TE_{14}	127.339	3.962	4.703	4.49[−2]	4.14[+2]	5.14

TABLE IV. Parameters for fifth-harmonic converters with beam energies lower than 200 kV. For all cases the beam velocity ratio $W/U=4.0$. The lengths $L_{50\%}$ to achieve an electronic efficiency of 50% (according to linear theory) and the corresponding power levels are for a beam current of 1 A. (Figures in brackets are powers of 10.)

Energy (kV)	Width a (cm)	B field (kG)	R (cm)	$k_{\parallel}$ (cm^{-1})	$K_5(k_\perp R)$	$P(L)/(I_0L)^2$ $W/(A\,cm)^2$	$L_{50\%}$ (cm)	Power (kW)
50	0.4811	7.295	0.1027	1.971	0.0168	1.47[+2]	13.0	25
70	0.4820	7.529	0.1188	2.272	0.0279	3.50[+2]	10.0	35
100	0.4830	7.883	0.1375	2.618	0.0435	7.36[+2]	8.2	50
150	0.4845	8.476	0.1601	3.029	0.0669	1.49[+3]	7.1	75
200	0.4857	9.073	0.1763	3.320	0.0849	2.17[+3]	6.8	100

energies down to 50 kV. The interacting waveguide mode in each case is TE_{03} circular polarization in square waveguide. The table gives the waveguide dimensions a, the magnetic fields B, the gyration radii R, the axial wave numbers $k_{\parallel}$, the fifth-harmonic coupling factors $K_5(k_\perp R)$, and the power growth rates $P(L)/(I_0L)^2$. Also shown are the interaction lengths $L_{50\%}$ required to reach a harmonic conversion efficiency of 50% for a 1-A beam current, together with the output powers in each case.

VI. DISCUSSION AND CONCLUSIONS

A derivation has been presented for the first-order power transfer into the fields of a TE_{lm} mode rectangular waveguide from a relativistic electron beam carrying spatiotemporal modulation. This work extends a previously published paper [1] that is limited to TE_{0m} modes [11] and is not competent to treat non-axis-encircling orbits, circularly polarized excitations, and competing modes. The present paper considers an idealized electron beam, free of momentum or guiding-center spreads, in order to bring out the essential physics of this class of interactions.

The general result found for the power transfer from the beam to the fields of a TE_{lm} mode waveguide is similar to that found for the TE_{0m} mode. Thus cumulative power flow from the beam to the fields of a selected waveguide mode is shown to occur when *both* frequency and wave-number matching occur, i.e., when the frequency for the interacting waveguide mode is equal to an integer multiple of the beam modulation frequency *and* when the wave-number of the mode is equal to the same integer multiple of the beam modulation pitch number. In the present work geometric coupling factors are derived [Eqs. (14) and (15)] that account for the guiding center location of the beam and the particular symmetry properties of the waveguide mode. When certain specific symmetries prevail, the power transfer is found to be identical for TE_{lm} modes as for TE_{0m}, except that the former can be a factor of 2 stronger than the latter, due to the presence of two electric-field components rather than one.

Power transfer from the beam to the waveguide fields is shown to occur in synchrony with an externally applied input field. However, it is also shown that power transfer occurs even in the absence of an external field. In this latter case, and when wave-number matching prevails at one of the temporal harmonics of the beam modulation frequency, the power level grows quadratically with both the interaction length and the dc beam current. When perfect wave-number matching does not occur the power transfer is reduced by a phase-interference factor, such as $(\sin\theta/\theta)^2$, where θ is half the total phase mismatch along the interaction length.

The aforementioned geometric coupling factors lead to selection rules for systems of sufficient symmetry. Thus for axis-encircling beams it is found that only odd temporal harmonics are excited in a TE_{0m} mode when m is odd, and only even temporal harmonics are excited when m is even. For axis-encircling beams exciting TE_{mm} modes in a square waveguide it is found that power transfer only occurs at even temporal harmonics, and that harmonics $s=2,6,10,\ldots,(4n-2),\ldots$ are excited when m is odd while harmonics $s=4,8,12,\ldots,(4n),\ldots$ are excited when m is even. For axis-encircling beams in a rectangular waveguide, conditions are derived as given by Eqs. (27)–(30) which allow the dimensions of the waveguide to be selected to maximize coupling at a given harmonic in a desired mode. In a square waveguide, where circularly polarized TE_{0m} modes can be supported, the power transfer rate is shown to be twice that for linearly polarized TE_{0m} modes for odd temporal harmonics (m odd), but equal to that for linearly polarized modes for even harmonics (m even). For circularly polarized odd-harmonic excitations the sense of rotation is shown to be counterclockwise for $s=1,5,9,\ldots,(4n+1),\ldots$ and to be clockwise for $s=3,7,11,\ldots,(4n-1),\ldots$. For non-axis-encircling beams it is shown that in general both even and odd temporal harmonics can be excited in any TE_{lm} mode. However, for TE_{mm} modes in a square waveguide, off-axis guiding center locations can be found for which power transfer is absent at all odd harmonics and at every other even harmonic.

Examples are given to illustrate the applicability of the theory in the conceptual design of converters to furnish fifth-harmonic power at 94 GHz. Such converters could offer attractive alternatives to conventional gyrotrons since the factor-of-5 reduction in the magnetic field required would obviate the need for a superconducting magnet system. Further advantages for the harmonic conversion mechanism, as discussed in I, could include low wall heat loading, low power collector demands, and no need for open mode converters as millimeter-wave

gyrotrons. The examples given in this paper show that respectable power transfer rates occur for the TE_{32} mode in rectangular waveguide, and for the TE_{03} mode supporting circular polarization in a square waveguide. However, mode competition is shown to be a serious issue for the TE_{32} case, particularly at the fourth and sixth harmonics. These effects are strongly suppressed in the square waveguide TE_{03} case, due mainly to the sparse mode spectrum of the square waveguide. The example demonstrates that power at the 100-kW level can be extracted from a 1-A, 200-kV spatiotemporally modulated beam in an interaction length of only several centimeters.

Fifth-harmonic operation at beam energies lower than 200 kV is also briefly described. It is found that respectable power growth rates exist for 1-A beams with energies as low as 50 kV, and that power levels at 94 GHz of several tens of kilowatts can be generated in interaction lengths of about 10 cm. These results could have practical significance for systems applications where higher beam energies are not desired due to the need for x-ray shielding. A figure of measure to compare results for conceptual devices with lower beam energies is taken to be the length $L_{50\%}$ at which half the dc beam power is predicted to be converted to radiation. This assumes that the linear theory developed in this paper can be used in what is clearly a strongly nonlinear regime, a point discussed in I. What is envisioned to make this possible is a gradually tapered-down magnetic field in the interaction region that maintains the phase matching between the beam and the fields, even as significant beam power is converted to rf power. The feasibility of this strategy has been examined in an approximate nonlinear analysis of the coupling mechanism [8], and is currently the subject of a more exact numerical simulation study [9]. Results of these studies show that the conversion of transverse energy from the beam to the fields can be highly efficient, as was speculated in I. Furthermore, while the power transfer rate does decrease as the rf power level increases along the interaction region, the length for transfer of half the available power was shown in several examples to be only about 10% greater than the length calculated from linear theory. Of course the precise difference between linear and nonlinear values of $L_{50\%}$ will depend upon the initial beam energy and other factors. Nevertheless, the preliminary nonlinear results cited here appear to give sufficient justification for using the linear values of $L_{50\%}$ as a measure of the strength of the interaction when comparing different cases.

Aside from a full study of the nonlinear aspects of this interaction, other issues which need to be addressed include the effects of momentum and gyration center spreads on the power transfer rates. Space-charge forces are expected to degrade the spatiotemporal modulation on the beam from the ideal form assumed in this paper, particularly for high perveance beams. In addition, coupling to TM modes needs to be examined as well, since it can be expected that these could lead to cumulative extraction of both longitudinal and transverse momentum from the beam. Furthermore, a full treatment of mode competition is not possible if, as in the present paper, only TE modes are considered. Extension of this work to higher energy beams and higher harmonic interactions should be straightforward, although the mode competition issue might be expected to intensify as the waveguide mode indices increase. A parallel study for modes in cylindrical waveguides would also be of interest, since there all modes can be excited in circular polarization, and since fabrication of experimental devices with cylindrical elements is usually preferred over devices with square elements. Mode competition issues should be comparable for cylindrical and square waveguide systems, since their spectral mode densities are essentially equal.

In conclusion, this paper has extended the previously published analysis to the full panoply of TE modes in a rectangular waveguide. Selection rules and phase-matching conditions are developed to allow the conceptual design of devices that cumulatively convert spatiotemporal modulation from an electron beam into millimeter wave radiation. Power levels in the range of 100 kW at 94 GHz appear to be achievable using a 200-kV, 1-A beam in a fifth-harmonic device with an interaction length of about 10 cm. Circularly polarized modes appear to be relatively free of mode competition. Lower-beam-energy devices are also shown to be capable of fifth-harmonic operation, albeit with lower output power.

ACKNOWLEDGMENTS

Helpful discussions with C. M. Armstrong, A. K. Ganguly, V. L. Granatstein, P. Malouf, and G. S. Park are acknowledged. Appreciation is extended to G. S. Park for producing Fig. 1. This research was supported by the Office of Naval Technology in collaboration with the Naval Research Laboratory.

APPENDIX: COUPLING OF SPATIOTEMPORALLY MODULATED BEAMS TO CIRCULARLY POLARIZED TE_{0m} MODES

For a square waveguide of side a the electric field is taken to be

$$\mathbf{E}(x,y,z,t)=E_0(z)[\hat{\mathbf{e}}_x \sin(k_m y)\sin\theta + \hat{\mathbf{e}}_y \sigma \sin(k_m x)\cos\theta] , \tag{A1}$$

where $k_m = m\pi/a$, $\theta = k_\parallel z - \omega t$, and $\sigma = \pm 1$, corresponding to clockwise $(+1)$ and counterclockwise (-1) rotation of the fields. The amplitude $E_0(z)$ is slowly varying with z. The equilibrium current density of the beam is given by Eqs. (1) and (2). The instantaneous power flow is

$$P(z,t)=\frac{1}{Z_{\mathrm{TE}}}\int_0^a dx \int_0^a dy (E_x^2+E_y^2)=\frac{a^2}{2Z_{\mathrm{TE}}}E_0^2(z) , \tag{A2}$$

which is seen to be independent of time, as is usual for circular polarization. From Eq. (A2) it follows that

$$\frac{dP(z,t)}{dz}=\frac{a^2}{Z_{\mathrm{TE}}}E_0(z)\frac{dE_0(z)}{dz} . \tag{A3}$$

But, in addition, we have

$$\frac{dP(z,t)}{dz}=-\int_0^a dx\int_0^a dy(J_{0x}E_x+J_{0y}E_y)\ . \tag{A4}$$

As in Sec. II, Eqs. (A3) and (A4) will be equated to find $dE_0(z)/dz$.

Substituting from Eqs. (A1), (1), and (2) into Eq. (A4) and integrating over x and y gives

$$\frac{dP(z,t)}{dz}=I_0\frac{W}{U}E_0(z)\times\left\{-\sin\theta\sin\phi\sin[k_m y_0+k_m R\sin\phi]+\sigma\cos\theta\cos\phi\sin[k_m x_0+k_m R\cos s\phi]\right\}. \tag{A5}$$

For an axis-encircling beam we have

$$\sin(k_m x_0)=\sin(k_m y_0)=\sin(m\pi/2)=\begin{cases}(-1)^{(m-1)/2}, & m \text{ odd}\\ 0, & m \text{ even}\end{cases}$$

and

$$\cos(k_m x_0)=\cos(k_m y_0)=\cos(m\pi/2)=\begin{cases}(-1)^{m/2}, & m \text{ even}\\ 0, & m \text{ odd}\ .\end{cases}$$

Thus

$$\sin[k_m y_0+k_m R\sin\phi]=\begin{cases}(-1)^{(m-1)/2}\sum_{n=0}^{\infty}\epsilon_n J_{2n}(k_m R)\cos 2n\phi, & m \text{ odd}\\ (-1)^{m/2}\sum_{n=0}^{\infty}2J_{2n+1}(k_m R)\sin(2n+1)\phi, & m \text{ even}\ ,\end{cases}$$

while

$$\sin[k_m x_0+k_m R\cos\phi]=\begin{cases}(-1)^{(m-1)/2}\sum_{n=0}^{\infty}\epsilon_n(-1)^n J_{2n}(k_m R)\cos 2n\phi, & m \text{ odd}\\ (-1)^{m/2}\sum_{n=0}^{\infty}2(-1)^n J_{2n+1}(k_m R)\cos(2n+1)\phi, & m \text{ even}\ .\end{cases}$$

Substituting these expressions into Eq. (A5) gives

$$\frac{dP(z,t)}{dz}=I_0\frac{W}{U}E_0(z)(-1)^{(m-1)/2}\sum_{n=0}^{\infty}\epsilon_n J_{2n}(k_m R)[-\sin\theta\sin\phi+\sigma(-1)^n\cos\theta\cos\phi]\cos 2n\phi \tag{A6}$$

for m odd, and

$$\frac{dP(z,t)}{dz}=I_0\frac{W}{U}E_0(z)(-1)^{m/2}\sum_{n=0}^{\infty}2J_{2n+1}(k_m R)[-\sin\theta\sin\phi\sin(2n+1)\phi+\sigma(-1)^n\cos\theta\cos\phi\cos(2n+1)\phi] \tag{A7}$$

for m even. After manipulation of Eqs. (A6) and (A7) we equate the results to Eq. (A3) to give

$$\frac{dE_0(z)}{dz}=2I_0\frac{W}{U}\frac{Z_{\rm TE}}{a^2}\sigma(-1)^{(m-1)/2}\times\sum_{n=0}^{\infty}(-1)^n K_{2n+1}(k_m R)\times\cos[\theta+\sigma(-1)^n(2n+1)\phi] \tag{A8}$$

for m odd, and

$$\frac{dE_0(z)}{dz}=2\sqrt{2}I_0\frac{W}{U}\frac{Z_{\rm TE}}{a^2}(-1)^{m/2}\times\sum_{n=0}^{\infty}K_{2n}(k_m R)\cos 2n\phi\sin[\theta+\sigma(-1)^{n-1}\frac{\pi}{4}] \tag{A9}$$

for m even, where $K_s(b)=(\epsilon_s/2)J_s'(b)$.

We now average Eqs. (A8) and (A9) over the time of interaction $T=\gamma z/U$. This requires a different manipulation for each expression. For Eq. (A8), we require the integral

$$I_1(z)=\frac{1}{T}\int_0^T dt\cos[A(z)+Bt]\ ,$$

where $A(z)=k_\parallel z+\sigma(-1)^n(2n+1)(\xi z+\phi_0)$ and $B=\omega+\sigma(-1)^n(2n+1)p$. This integral is seen to approach zero as z increases unless the matching condition $\omega+\sigma(-1)^n(2n+1)p=0$ is met. Thus for even n, corresponding to harmonics $s=1,5,9,13,\ldots,(4j+1),\ldots$ we have $\sigma=-1$ (counterclockwise sense of rotation), while for odd n, corresponding to harmonics $s=3,7,11,15,\ldots,(4j-1),\ldots$ we have $\sigma=+1$ (clockwise sense of rotation). When these matching conditions are met the above integral goes over to $I_1(z)=\cos A(z)$.

For Eq. (A9) we require the integral

$$I_2(z)=\frac{1}{T}\int_0^T dt\,\cos(2n\phi)\sin[\theta+\sigma(-1)^{n-1}\pi/4]\ .$$

If we drop the small antiresonant part of $I_2(z)$ we have

$$I_2(z)=\frac{1}{2T}\int_0^T dt\,\sin[A'(z)-B't]\ ,$$

where $A'(z)=(k_\parallel-2n\xi)z-2n\phi_0+\sigma(-1)^{n-1}\pi/4$ and $B'=\omega-2np$. The integral will tend towards zero as z increases unless $B'=0$. Thus for all even harmonics $\omega=2np$, we have $I_2(z)=[\sin A'(z)]/2$.

The time-averaged values of Eqs. (A8) and (A9) are thus

$$\left\langle\frac{dE_0(z)}{dz}\right\rangle=2I_0\frac{W}{U}\frac{Z_{\rm TE}}{a^2}(-1)^{(m-1)/2}\times K_{2n+1}(k_mR)\cos A(z) \tag{A10}$$

for $\omega=(2n+1)p$, and

$$\left\langle\frac{dE_0(z)}{dz}\right\rangle=\sqrt{2}I_0\frac{W}{U}\frac{Z_{\rm TE}}{a^2}(-1)^{m/2}K_{2n}(k_mR)\sin A'(z) \tag{A11}$$

for $\omega=2np$. Integration over z in Eq. (A10) involves the integral

$$I_3=\int_0^L dz\,\cos A'(z)$$

$$=L\left\{\cos b_1\left[\frac{\sin(a_1L)}{a_1L}\right]+\sin b_1\left[\frac{\cos(a_1L)-1}{a_1L}\right]\right\},$$

where $a_1=k_\parallel+\sigma(-1)^n(2n+1)\xi$ and $b_1=\sigma(-1)^n(2n+1)\phi_0$. I_3 will be small unless $a_1L=0$. This is seen to require observance of the same selection rules for rotation as in the time averaging above, in which case $I_3=L\cos b_1$. Similarly, integration over z in Eq. (A11) involves the integral

$$I_4=\int_0^L dz\,\sin A(z)$$

$$=L\left\{\cos b_2\left[\frac{1-\cos(a_2L)}{a_2L}\right]+\sin b_2\left[\frac{\sin(a_2L)}{a_2L}\right]\right\},$$

where $a_2=(k_\parallel-2n\xi)$ and $b_2=\sigma(-1)^{n-1}\pi/4-2n\phi_0$. Again, we see that I_4 will be small unless $a_2L=0$, in which case $I_4=L\sin b_2$. This requires observance of the same matching condition as in the evaluation of $I_2(z)$, irrespective of the sense of wave rotation. Once the relative phase angle ϕ_0 adjusts to the value that maximizes the power transfer we find the results given in Eqs. (32) and (33).

[1] J. L. Hirshfield, Phys. Rev. A **44**, 6845 (1991).

[2] R. Shpitalnik, C. Cohen, F. Dothan, and L. Friedland, J. Appl. Phys. **70**, 1101 (1991).

[3] D. B. McDermott, D. S. Furono, and N. C. Luhmann, Jr., J. Appl. Phys. **58**, 4501 (1985).

[4] C. S. Kou, D. B. McDermott, N. C. Luhamann, Jr., and K. R. Chu, IEEE Trans. Plasma Sci. **18**, 343 (1990).

[5] Y. Y. Lau, M. Friedman, J. Krall, and V. Serlin, IEEE Trans. Plasma Sci. **18**, 553 (1990).

[6] A. C. McCurdy, C. M. Armstrong, W. M. Bollen, R. K. Parker, and V. L. Granatstein, Phys. Rev. Lett. **57**, 2379 (1986); W. Lawson *et al.*, Phys. Rev. Lett. **67**, 520 (1991).

[7] P. Malouf and V. L. Granatstein, Int. J. Electron. **72**, 943 (1992).

[8] J. L. Hirshfield (unpublished).

[9] A. K. Ganguly (private communication).

[10] *Handbook of Mathematical Functions,* edited by M. Abramowitz and I. A. Stegun (Dover, New York, 1965), pp. 231–243.

[11] The definition of $K_m(k_\perp R)$ given in I differs from that given in this paper, on account of an incorrect interchange in Eq. (13) of I between the phase angles in momentum and configuration space. [The factor $\cos\phi'$ in Eq. (13) of I should have been $-\sin\phi'$, as in Eq. (1) of this paper.] This does not alter the results of I from Eq. (17) on, except in redefining $K_m(k_\perp R)=(\epsilon_m/2)J'_m(k_\perp R)$. The entire correct derivation for the case of TE_{0m} modes may be found from the present paper by setting $\alpha=\pi/2$. In Table II of I correct values of K_m should be 0.1013 and 0.069 48, while the correct values of $P_m(L)/L^2$ should be 7.69 and 0.403 kW/cm^2. In Table III of I the correct value of K_m is 0.008 13 [from the asymptotic relationship for large m, $J'_m(m)\sim 0.410\,85\ m^{-2/3}$], while the correct value of output power at $L=30$ cm is 1.84 kW. [See also, J. L. Hirshfield, Phys. Rev. A **46**, 2188 (E) (1992).]